CONF-780912--1

PREPRINT UCRL- 80725

Lawrence Livermore Laboratory

NONCONTACT MATERIAL TESTING USING LASER ENERGY DEPOSITION AND INTERFEROMETRY

Clarence A. Calder
William W. Wilcox

February 6, 1978

This paper was prepared for submission to

Proceedings of Sixth International Conference on Experimental Stress Analysis, European Permanent Committee for Stress Analysis, Munich, Germany, Sept. 18-22, 1978

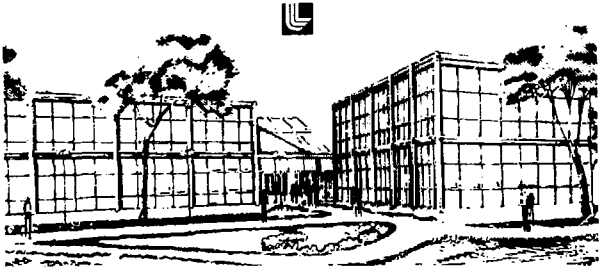

NONCONTACT MATERIAL TESTING USING LASER ENERGY DEPOSITION AND INTERFEROMETRY

by

Clarence A. Calder
William W. Wilcox

Lawrence Livermore Laboratory
Livermore, California 94550

ABSTRACT

A technique is described for the noncontact testing of materials using laser deposition to generate a stress pulse and interferometry to record the transient surface displacement. The dilatational wave speed can be measured and, in the particular case of rod or plate specimens, sufficient information can be obtained to evaluate the two elastic constants of an isotropic material. Several applications illustrating the advantages of the approach are summarized.

1. Introduction

The accurate characterization of material behavior for use in computer models and calculations is continually required for the design of safe and efficient structures and machine components. Frequently, new materials or unique applications require measurements of material properties where conventional methods are unsuitable. In this work, an experimental technique is described which allows loading of a specimen and the recording of its dynamic response without physical contact with the specimen. The transient load is applied by rapid energy deposition from a Q-pulsed, high energy laser. The rapid heating produces vaporization of the surface skin and the resulting blowoff drives a compressive stress pulse into the material. Stress wave arrivals are monitored using a dynamic displacement interferometer.

In a number of situations this technique has distinct advantages over the commonly used ultrasonic methods. The laser loading produces a large stress pulse amplitude of short duration so that tests of highly attenuating or very thin materials are possible. The short measurement time of a few microseconds or less can be made at a precise instant in time. The noncontact feature is especially useful for testing in severe environments and with toxic materials. There are few restrictions on specimen size and configuration and the specimen can be far removed from the instrumentation hardware. In addition, tests have shown that flat and specular surfaces are often not necessary for adequate interferometry measurements.

2. Specimen Loading by Laser Energy Deposition

The potential for generating stress waves in materials by laser energy deposition has been recognized since the early sixties following the invention of the pulsed ruby laser in 1960. Ready [1] gave one of the first treatments describing the effects of normal mode and Q-switched laser pulses absorbed at opaque surfaces. In the late sixties, Percival [2] conducted a study of laser generated stress waves in an absorbing rod and used Pochhammer-Chree theory to describe the dynamic stress reponse. This approach was used to determine the elastic constants of rod specimens at elevated temperatures using a sandwiched

piezoelectric tourmaline crystal [3]. Skeen and associates [4] used quartz stress gages to record stress pulse amplitudes created by the rapidly expanding plasma. A following study [5] explored the large plastic deformation of thin plates subjected to laser loading with the plasma confined by a surface overlay. Laser induced stress pulses with rise times of less than 1 ns and half-amplitude durations of 3 ns have been produced with a 3-ps pulsed laser [6]. More recently, Krehl, Schwirzke, and Cooper [7] have made measurements to show plasma momentum from aluminum targets to be in reasonably good agreement with the measured target impulse obtained from quartz gage data. Fairand and coworkers have conducted several studies [8,9,10] related to increased laser generated stress amplitudes by using surface overlays. They produced extensive plastic flow at the surface of an iron-silicon alloy specimen but found the stress amplitude decayed rapidly as it progressed into the interior. An extensive coverage of work done up to 1971 on material response to high power lasers is given by Ready. [11]

Much effort is currently being expended in laser-material interaction studies ranging from metal scribing at low energy to laser fusion at ultra high energy. At moderate laser-energy levels, stress pulse amplitudes on the order of the yield stress of metals can be reached. Such stress waves are induced by at least two mechanisms, and depending on the opacity of the material to the laser wavelengh used, one mechanism or the other may predominate. In the first, the rapid deposition of laser energy into an absorbing material produces a state of unbalanced, compressive thermal stress as the heated material wants to expand but is restrained initially by its own inertia. This stress gradient propagates into the material and is immediately followed with a tensile tail arising from the front surface reflection. See, for example, Ref. 12.

In the second mechanism, an opaque target surface is rapidly vaporized by the high energy laser pulse, and the recoil from blowoff of the vapor causes a strong, transient pressure build-up. The pressure on the target surface induces a compressive stress pulse that propagates through the material. This mechanism is illustrated in Fig. 1 which shows the laser generated plasma blowoff from a 6.35-mm-thick aluminum disk subjected to laser deposition from a neodymium-glass laser pulse of about 12 J and 30 ns

acting on a 22-mm-dia. area.

The second mechanism does produce some surface damage but in most cases it is undetectible except for a slightly scorched appearance of the surface. The results of laser deposition on a 25-mm-diam aluminum disk at three energy densities are shown in the upper left of Fig. 2. The disk surface was first prepared with 600 grit sandpaper to provide a reasonably uniform surface roughness. Then the surface was exposed to 1.06 μm laser pulses of (A) 5 J and (B) 12 J over a 10-mm-diam area, and (C) 12 J focused to about 1 mm diameter. The latter produced a clearly evident crater in the surface. Scanning electron microscopy views of the original and exposed surface (B) are shown at 1000X. The vaporization and melting of the ridge peaks are evident in the upper right view of Fig. 2.

Measurements of actual material mass removed by laser deposition were taken for three samples each of four metals and the average surface depth removed calculated. The laser energy used was 12 J at 1.06 μm and 30 ns over a spot about 10 mm in diameter. The results, tabulated in Table 1, show the actual depth removed to be extremely small.

Surface overlays, such as highly absorbing black paint or a transparent sheet of slide glass, have been known to greatly effect the amplitude and duration of the stress pulse induced in the specimen. In cases where the overlay is highly absorbing, a larger percentage of the laser energy is absorbed creating a greater blowoff pressure. When a transparent overlay (tamper) is used, the laser energy is absorbed at the specimen surface and the confined plasma produces a much higher pressure. The effect was explored by conducting laser deposition tests on a 6.35-mm-thick aluminum disk specimen with the following surface conditions:

1) bare and cleaned by previous shots,
2) blacked with a felt tip pen,
3) tampered with cellophane tape,
4) blacked and tampered with tape.

Laser deposition from a Q-pulsed neodymium-glass laser operating with a 12 J and 30 ns pulse duration was spread approximately uniformly over an area of 22 mm diam in each case. Stress arrival at the back face was monitored with an acoustically-matched quartz transducer with a 10-mm-diam guard ring using the technique described by Graham. [13] This one-dimensional strain experiment permitted recording of the complete laser induced compressive pulse before edge effects

invalidated the quartz transducer output.

Stress profile results for the four surface conditions are compared in Fig. 3. While blacking the surface nearly doubled the peak stress of the bare surface, the taped overlay produced a ten-times increase in stress amplitude. As expected, the maximum stress of about 157 MPa was achieved with the combined blacked and taped surface. The half-amplitude stress pulse duration decreased from 240 ns for the bare surface to 95 ns for the blacked and taped condition. Rise time was about 45 ns in all cases. Earlier work [14] has shown the transparent cellophane tape to be as effective in enhancing the stress amplitude as more massive and less convenient transparent overlays of quartz, epoxy, and slide glass. Possibly the adhesive backing has a significant influence on the pressure developed.

3. Specimen Response By Laser Interferometry

Most work with laser deposition loading has been recorded using piezoelectric quartz transducers. These devices are very sensitive, have high frequency response, and in the case of one-dimensional strain or stress experiments, can provide accurate stress-time data. However, there are several obvious limitations to their use in general. First, the specimen must have flat surfaces to permit direct contact and good coupling with the transducer. Second, specimen size limitations are governed by the transducer size and possible overlapping of the original and echo stresses in the specimen. Third, in general the transducer is not acoustically matched to the specimen material requiring corrections to be made in the data to obtain accurate stress information. Finally, these transducers do not survive well in severe environments and their piezoelectric character disappears at high temperatures.

These limitations are overcome and completely noncontact testing made possible by using a Michelson displacement interferometer to sense the stress wave arrivals at the back face of the specimen. Although the normal stress of the free surface is always zero, the displacement and velocity are nonzero at the time the stress pulse is reflecting from the back face. The specimen surface becomes the moving mirror of the interferometer. When light reflected from the specimen surface is recombined with light from the reference mirror, a series of light and dark bands or fringes are produced. Surface motion of the specimen causes fringe movement which can be

monitored by a photodector.

A schematic of the interferometric arrangement used is shown in Fig. 4 and is similar to that described by Barker and Hollenbach, [15] The output from a single frequency, Spectra Physics model 164 argon-ion laser, operated at a wavelength of 0.5145 μm, is directed to a beam splitter positioned at 45 degrees to the beam. The specimen and reference mirror, placed perpendicular to each other and equidistant from the beam splitter, reflect the split beams back to the beam splitter where they are recombined to from a pattern of concentric, circular fringes. The fringe pattern can be observed during setup by placing a screen at the photodetector.

The photodetector is an RCA model 7326 ten-stage photomultiplier tube and associated circuitry. The circuit is designed to provide up to 10 V of linear output from the photomultiplier tube. The tube is in an "off" mode when the high voltage is on until a turn-on trigger signal of 25 V is applied. This feature permits operation with the high ambient light level present and provides much higher sensitivity at the moment the desired signal occurs.

The fringe pattern is enlarged with an expanding lens so that the photodetector, equipped with a 0.7-mm-diam aperature, senses only one fringe at a time at the center of the bulls-eye pattern. Movement of the free surface a distance equal to one-half the wavelength of the laser ($\lambda/2$) causes the center of the concentric fringe pattern to change from light to dark to light. Thus, the detector output is a frequency modulated sine wave with each successive peak representing an additional surface displacement of $\lambda/2$. This is illustrated by the simulated trace in Fig. 4 showing the photomultiplier circuit turn-on at (1) to a d-c voltage level representing the fringe position at that instant of time. Specimen movement causes a sine wave type output beginning at (2) with each complete cycle representing a specimen back surface displacement of 0.2572 μm. For perfect fringe contrast, the valleys of the output would return to the zero voltage level at (1) indicating complete light extinction. In cases where the specimen surface is not a good mirror this desired condition is difficult to achieve. In these cases fringe contrast can be improved by focusing the specimen beam to a point on the

specimen surface and using a neutral density filter in the reference leg to equalize intensities of the recombined beams. A 0.5145 μm spike filter is placed in front of the photomultiplier tube aperture to filter out unwanted pulsed light from the high energy laser, flash tube, and laser generated plasma.

4. Noncontact Testing Arrangement

The combination of pulsed laser energy deposition for specimen loading and laser displacement interferometry for measuring specimen response provides a unique setup for noncontact testing of materials in a number of situations which would be impossible or very difficult using more conventional approaches. A schematic of the noncontact test arrangement is shown in Fig. 5. Specimen loading is accomplished by laser deposition on the specimen surface from a Q-switched Holobeam series 6082 neodymium-glass laser at energies up to 15 J. Half-amplitude pulse duration is typically about 20-30 ns. A slide glass beam splitter is used to direct a small portion of the input beam to a 0.5-ns-risetime Monsanto silicon pin photodiode model MD2. The output of the photodiode circuit, about 10 V, is used to trigger the oscilloscope time base or a digital delay plug-in unit which triggers the trace after a preset time delay. Signals were recorded on a Tektronix 7904 oscilloscope using a 7A19 plug-in amplifier and a 7B92A dual time base resulting in a 500 MHz bandwidth capability. A 15 mW Spectra Physics model 124 helium-neon laser is used for precise alignment of the high energy laser and the specimen. The components of the interferometer are as described in the previous section with the exception that in some earlier applications the helium-neon alignment laser was used in place of the argon-ion laser. This particular model is not single frequency and more than one axial mode may be generated. This causes the laser output beam to be amplitude modulated at the beat frequencies of the active axial modes and results in "noisy" data traces.

In experiments requiring accurate measurement of stress wave transit time through the specimen, where the transit time may be only a few hundred nanoseconds, inherent delays in the scope triggering and vertical input amplifier, transit time through the photomultiplier tube, electrical and optical path travel time, and effective

initiation time of the stress pulse must be known or excluded from affecting the data. The time of initiation of the stress pulse was measured by using a thin plate of high purity, oxygen-free copper of known dilatational velocity as the specimen in Fig. 5. A second slide-glass beam splitter was placed at the high energy input to provide a fiducial marker superposed on the photomultiplier signal output from the interferometer. This procedure eliminated all other timing considerations except the difference in optical path lengths which could be easily determined. The optical path from the fiducial beam splitter to the photomultiplier tube is 0.46 m shorter than the air path via the interferometer, so the high energy laser pulse appears 1.5 ns early on the oscilloscope record shown in Fig. 6. The transit time for the 0.91-mm-thick specimen is 192 ns based on a dilatational velocity of 4740 m/s for high purity copper. [16] Therefore, the time of initiation of the stress pulse is obtained by measuring back 190.5 ns from the breakout of the interferometer signal as shown in Fig. 6. The time of stress initiation was found to be very close to the half-amplitude point on the rise of the high energy laser pulse fiducial. The same conclusion was found, within ±5 ns, for similar tests on other metals.

Using the noncontact test arrangement, measurements of wave velocities accurate to 1-2% are possible. The scope sweep should be calibrated at the sweep rate used and corrections made for the various electrical and optical delays occurring in the particular setup. Transient displacements can be determined to within a fraction of a wavelength of the laser light used provided tilt of the specimen surface is small. The determination of stress from the displacement record would be considerably less accurate due to errors and difficulties inherent in differentiating experimental data. Velocity interferometry might be considered as an alternative, but is somewhat less sensitive. Also, a recent technique called a "velocity interferometer system for any reflector" (VISAR) [17] would provide velocity information directly as well as reduce the necessity for a good surface mirror and small tilt.

5. Applications

Several examples of noncontact testing will be briefly discussed to illustrate the technique and

give insight to potential applications which might be more conveniently done with this approach.

5.1 One-Dimensional Strain Experiment

Laser loading of reasonably uniform intensity over a sufficiently large area of a disk specimen induces a one-dimensional strain pulse into the material. This strain pulse quickly deteriorates to a complex state due to unloading waves propagating inward from the edge of the loading. Displacement interferometry on the back face of the specimen will indicate the arrival of the main disturbance, the arrival of its echo off the front face, and the deterioration of the one-dimensional strain state. Data records for two tests at different laser intensities are shown in Fig. 7 for a 53-mm-diam by 6.35-mm-thick aluminum disk. The laser energy of 9 J was spread over a 19 mm diameter in the first test and 50 mm diameter in the second. The expanded sweep in Fig. 7A indicates a pulse duration of about 100 ns. The record of Fig. 7B shows the first arrival, the echo or one-round-trip reflection 2.0 μs later, and the edge effect appearing an additional 0.1 μs later. The decrease in laser fluence from 0.1 to 0.015 GW/cm^2 reduced the back surface displacement by one-half.

5.2 Measurement of Elastic Constants

A longitudinal wave induced in one end of a rod will travel axially with grazing incidence to the rod lateral surface at the dilatational velocity with part of its energy continuously mode converted to shear waves. The shear wave travels at a slower velocity diagonally across the rod diameter to the opposite surface. There it mode converts back to a shear wave reflecting back into the material and to a dilatational wave again propagating at grazing incidence to the rod. This process is continually repeated resulting in a successive train of pulses arriving at the far end of the rod, the first appearing at the dilatational transit time with the following pulses delayed by a time related to the rod diameter and shear wave velocity. The measured time of arrival of the first two pulses along with the specimen dimensions and mass density provide sufficient information to calculate the elastic constants of the isotropic material using a single test. [18]

This ultrasonic test can be conducted using the

noncontact approach where the compressional pulse is induced in one end of the rod by laser energy deposition and the stress wave arrivals at the opposite end sensed with the displacement interferometer. The noncontact feature is especially convenient for high temperature material property measurement with the addition of a clamshell oven surrounding the specimen. [19] An actual oscilloscope trace showing the displacement response of a 6.35-mm-[illegible]y 101-mm-long tantalum rod at 200 C is illustrated in Fig. 8. The sweep was delayed 23.5 μs and swept at 500 ns per division. The arrival times of the dilatational and mode converted signals are clearly indicated. The values of t and Δt lead directly to the evaluation of the wave velocities and elastic constants of tantalum at 200 C.

5.3 Acoustic Velocity Measurement in Liquid Metal Column

An isobaric expansion apparatus has been developed to measure various thermophysical properties of liquid metals at very high temperatures and pressures. [20] In this experiment, a specimen the diameter of a common paper clip (1 mm) and about 25-mm long is subjected to rapid resistance heating by current dumped from a large capacitor bank. Required measurements are taken during an instant a few microseconds after specimen melt but before instability and breakup of the molten column takes place. An additional measurement of sound velocity across the diameter of the specimen at this instant in time would permit a more complete evaluation of the thermodynamic state of the liquid metal. Such a measurement by traditional means would be impossible. However, the noncontact approach is ideally suited for obtaining this information provided the liquid metal remains sufficiently reflective for the interferometric measurements.

The basic setup of Fig. 5 was used with optical access to the specimen through tapered sapphire windows positioned in the pressure cell wall on opposite sides of the vertical, 1-mm-diam specimen. The high energy laser was focused to a spot about 0.2-mm-diam on the lateral surface of the specimen and, diametrically opposite, the interferometer laser beam was focused. The specimen and anvil holder are shown in Fig. 9 with the high energy beam and generated plasma on the left and the interferometer laser beam on the right.

Lead specimens were selected to demonstrate the technique due to the relatively low energy required to obtain melt. Sonic velocity measurements were first made on solid lead rods and subsequently on lead rods liquified by the high current pulse from a 20 kV capacitor bank discharge. The stress transit time measurement was made a few microseconds following melt. Typical oscilloscope traces are shown in Fig. 10 for the solid and liquid lead runs. As in the stress initiation time measurement, Section 4, the fiducial marker is simply a representation of the timing of the high energy laser pulse. The measured sonic velocity for the solid specimen was reasonably close to an average value 2.21 mm/μs taken from Ref. [16]. As would be expected, there was a considerable drop in velocity for the liquid lead test. The measured liquid lead sound velocity of 1.80 mm/μs agreed very well with a published value at melt of 1.78 mm/μs. [21]

5.4 Flaw Detection

As in conventional ultrasonic testing, the noncontact approach can provide data on the presence and location of flaws in the material. To show this, a 1.5-mm-diam hole was drilled at the midthickness of a 25-mm thick aluminum plate to provide an artificial flaw as shown in Fig. 11. The interferometer was set up using the unpolished, as received, back surface and a stress pulse was induced by laser deposition. The oscilloscope trace clearly shows the arrival of the flaw induced echo as well as the first arrival and one-round-trip echo of the main pulse.

6. Conclusions

Noncontact material testing using laser deposition loading and displacement interferometry can provide accurate material response data. The technique is especially advantageous in situations where conventional methods are impossible or difficult to use.

References

(1) Ready, J.F., "Effects Due to Absorption of Laser Radiation", J. Appl. Phys., V. 36, No. 2, Feb. 1965, 462-468.

(2) Percival, C.M. and Cheney, J.A., "Thermally Generated Stress Waves in a Dispersive Elastic Rod", Exp. Mech., V. 9, No. 2, Feb. 1969, 49-57.

(3) Brammer, J.A. and Percival, C.M., "Elevated-Temperature Elastic Moduli of 2024 Aluminum Obtained by a Laser-pulse Technique", Exp. Mech., V. 10, No. 6, June 1970, 245-250.

(4) Skeen, C.H. and York, C.M., "Laser-induced 'Blow-off' Phenomena,", Appl. Phys. Letters, V. 12, No. 11, June 1968, 369-371.

(5) Skeen, C.H., et. al., "The Deformation of Thin Plates by Stress Waves Generated in Confined Laser Heated Plasmas", Sandia Laboratories, SC-CR-69-3306, Nov. 1969.

(6) Peercy, P.S., et. al., "Ultrafast Rise Time Laser-induced Stress Waves", Appl. Phys. Letters, V. 16, No. 3, Feb. 1970, 120-122.

(7) Krehl, P., Schwirzke, F. and Cooper, A.W., "Correlation of Stress-wave Profiles and the Dynamics of the Plasma Produced by Laser Irradiation of Plane Solid Targets", J. Appl. Phys., V. 46, No. 10, Oct. 1975, 4400-4406.

(8) Fairand, B.P., et. al, "Quantitative Assessment of Laser-induced Stress Waves Generated at Confined Surfaces", Appl. Phys. Letters, V. 25, No. 8, Oct. 1974, 431-433.

(9) Fairand, B.P. and Clauer, A.H., "Effect of Water and Paint Coatings on the Magnitude of Laser-generated Shocks", Optics Comm., V. 18, No. 4, Sept. 1976, 588-591.

(10) Clauer, A.H., Fairand, B.P. and Wilcox, B.A., "Pulsed Laser Induced Deformation in an Fe-3 Wt Pct Si Alloy", Metall. Trans. A V. 8A, Jan. 1977, 119-125

(11) Ready, J.F., Effects of High-power Laser Radiation, Academic Press, New York, 1971.

(12) Percival, C.M., "A Quantitative Measurement of Thermally Induced Stress Waves, AIAA J., V. 9, No. 2, Feb. 1971, 347-349.

(13) Graham, R.A., Neilson, B., and Benedick, W.B., "Piezoelectric Current from Shock Loaded Quartz - A Sub-microsecond Stress Gage", J. Appl. Phys., V. 36, No. 5, May 1965, 1775-1778.

(14) Wilcox, W.W., "Enhanced Stress Waves in Solids", Lawrence Livermore Laboratory, UCID-16447, Feb. 1974.

(15) Barker, L.M. and Hollenbach, R.E. "Interferometer Technique for Measuring the Dynamic Mechanical Properties of Materials", Rev. Sci. Instrum., V.36, No. 11, Nov. 1965, 1617-1620.

(16) Simmons, G. and Wang, H., Single Crystal Elastic Constants and Calculated Aggregate Properties: A Handbook, 2nd Ed., MIT Press, Cambridge, 1971.

(17) Barker, L.M. and Hollenbach, R.E., "Laser Interferometer for Measuring High Velocities of any Reflecting Surface", J. Appl. Phys., V. 43, No. 11, Nov. 1972, 4669-4675.

(18) Calder, C.A. and Wilcox, W.W., "Technique for Measurement of Elastic Constants by Laser Energy Deposition", Rev. Sci. Instrum., V. 45, No. 12, Dec. 1974, 1557-1559.

(19) Calder, C.A. and Wilcox, W.W., "High Temperature, Noncontact Material Testing", Lawrence Livermore Laboratory, UCRL-80438, Dec. 1977.

(20) Gathers, G.R., Shaner, J.W., Calder, C.A. and Wilcox, W.W., "Determination of Sound Velocity in Liquid Metals at Temperatures Greater than 4000 K", Proceedings of the Seventh Symposium on Thermophysical Properties, May 1977.

(21) Webber, G.M.B. and Stephens, R.W.B., "Transmission of Sound in Molten Metals", Physical Acoustics, W.O. Mason, Ed., V. IV - Part B, Academic Press, New York, 1968, 53-97.

"Work performed under the auspices of the U.S. Department of Energy by the Lawrence Livermore Laboratory under contract number W-7405-ENG-48."

Table 1. Weight of surface skin vaporized in laser deposition tests of four metals. Neodymium-glass laser, Q-pulsed with irradiance of 15 J/cm^2.

METAL	AVG WT LOST	AVG DEPTH REMOVED
1018 Steel	5 μg	0.008 μm
Aluminum	2 μg	0.010 μm
Tantalum	18 μg	0.014 μm
Nickel	25 μg	0.036 μm

FIGURE CAPTIONS

Fig. 1. Plasma blowoff from 6.35-mm-thick aluminum disk. Pulse was 12 J, 30 ns from neodymium-glass laser on 22-mm-diam area.

Fig. 2. Effect of laser deposition on aluminum. Laser energy density was about A) 6 J/cm^2. Background was unexposed surface at 1000X and upper right was area B at 1000X.

Fig. 3. Stress histories for four surface conditions.

Fig. 4. Displacement interferometer arrangement with simulated photomultiplier output trace.

Fig. 5. Schematic of noncontact testing arrangement using laser deposition loading and displacement interferometry.

Fig. 6. Data trace for determining time of stress initiation for 0.91 mm copper specimen.

Fig. 7. One-dimensional strain data for 53-mm-diam by 6.53-mm-thick aluminum disk at fluences of about A) 0.1 GW/cm^2 and B) 0.015 GW/cm^2.

Fig. 8. Displacement response of 6.35-mm-diam tantalum rod at 200 C and subjected to laser deposition on one end.

Fig. 9. Anvil mount and 1-m-diam specimen for liquid metal test with high energy and interferometer laser beams shown.

Fig. 10. Data for sound velocity measurement across the diameter of the A) solid lead and B) liquid lead specimens.

Fig. 11. Flaw detection using noncontact testing.

CALDER
Fig. 1

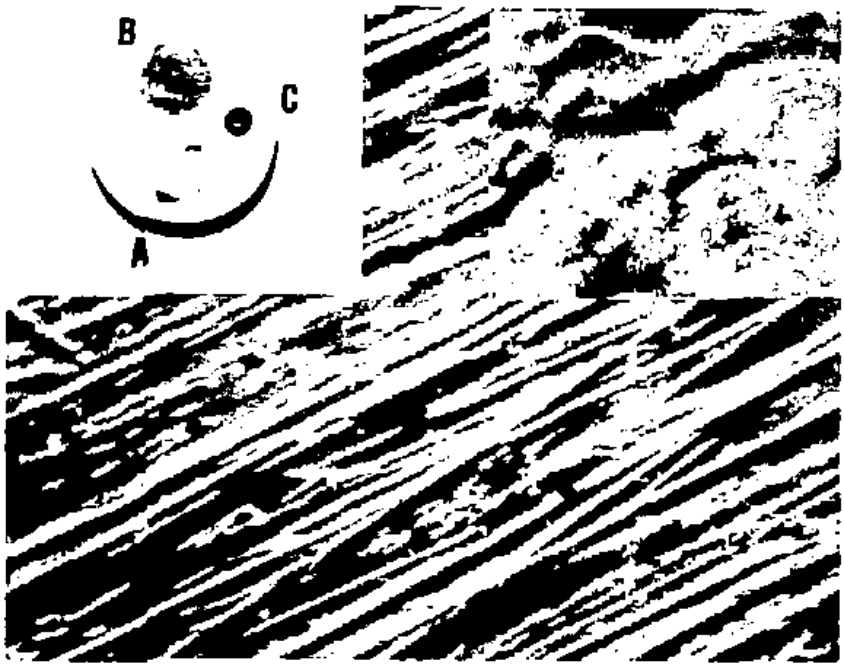

CALDER
FIG. 2

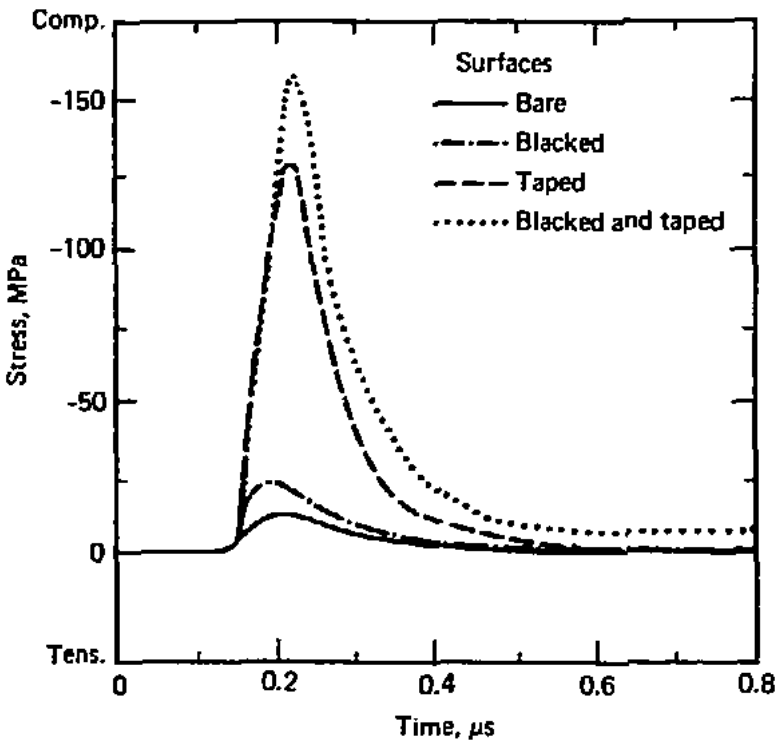
Comp.
-150
-100
-50
0
Tens.
Stress, MPa
Surfaces
Bare
Blacked
Taped
Blacked and taped
0
0.2
0.4
0.6
0.8
Time, μs

CALDER
Fig. 3

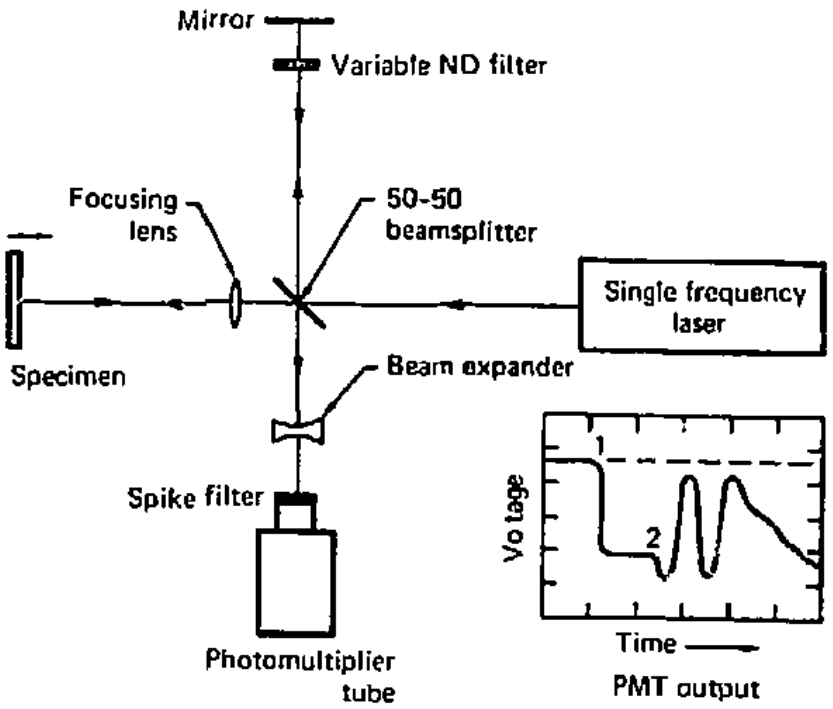
Mirror
Variable ND filter
Focusing lens
50-50 beamsplitter
Single frequency laser
Specimen
Beam expander
Spike filter
Photomultiplier tube
Voltage
1
2
Time
PMT output

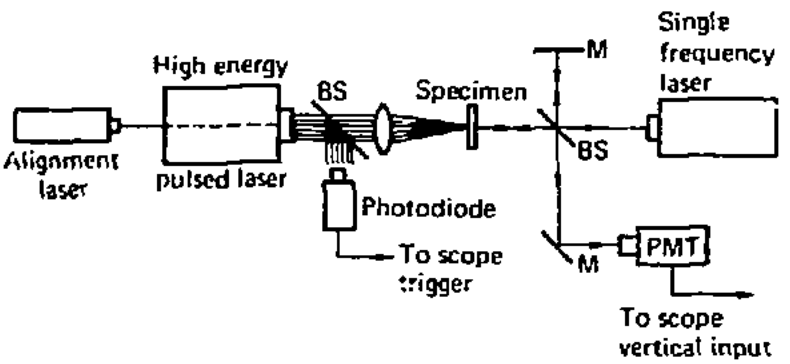
Single
frequency
laser
M
High energy
BS
Specimen
Alignment
laser
pulsed laser
BS
Photodiode
To scope
trigger
PMT
M
To scope
vertical input

Calda
Fig 5

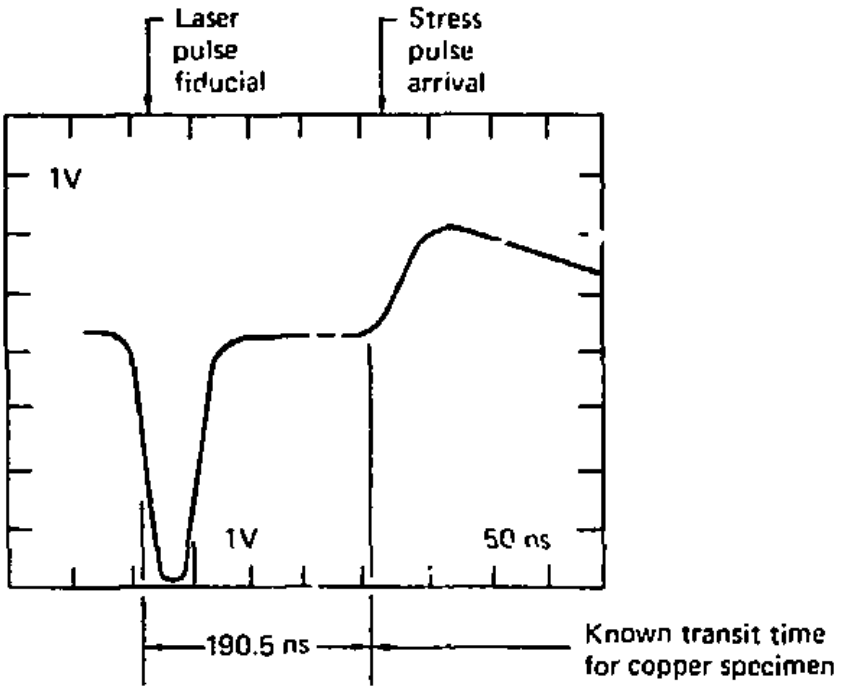
Laser
pulse
fiducial
Stress
pulse
arrival
1V
1V
50 ns
190.5 ns
Known transit time
for copper specimen

A. Response:
19 mm dia. deposition
(~0.1 GW/cm^2)

←→ ~100 ns

Displ. ≅ 0.45 μm

B. Response:
50 mm dia. deposition
(~0.015 GW/cm^2)

2.0 μsec
echo time ←——→

Displ. ≅ 0.22 μm

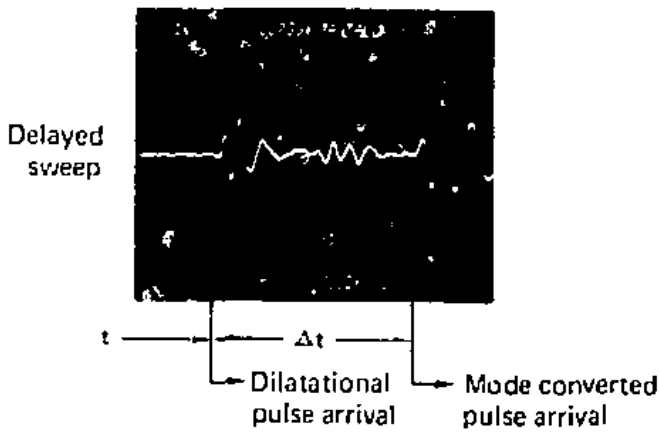
Delayed
sweep
t
Δt
Dilatational
pulse arrival
Mode converted
pulse arrival

CALDER
Fig. 8

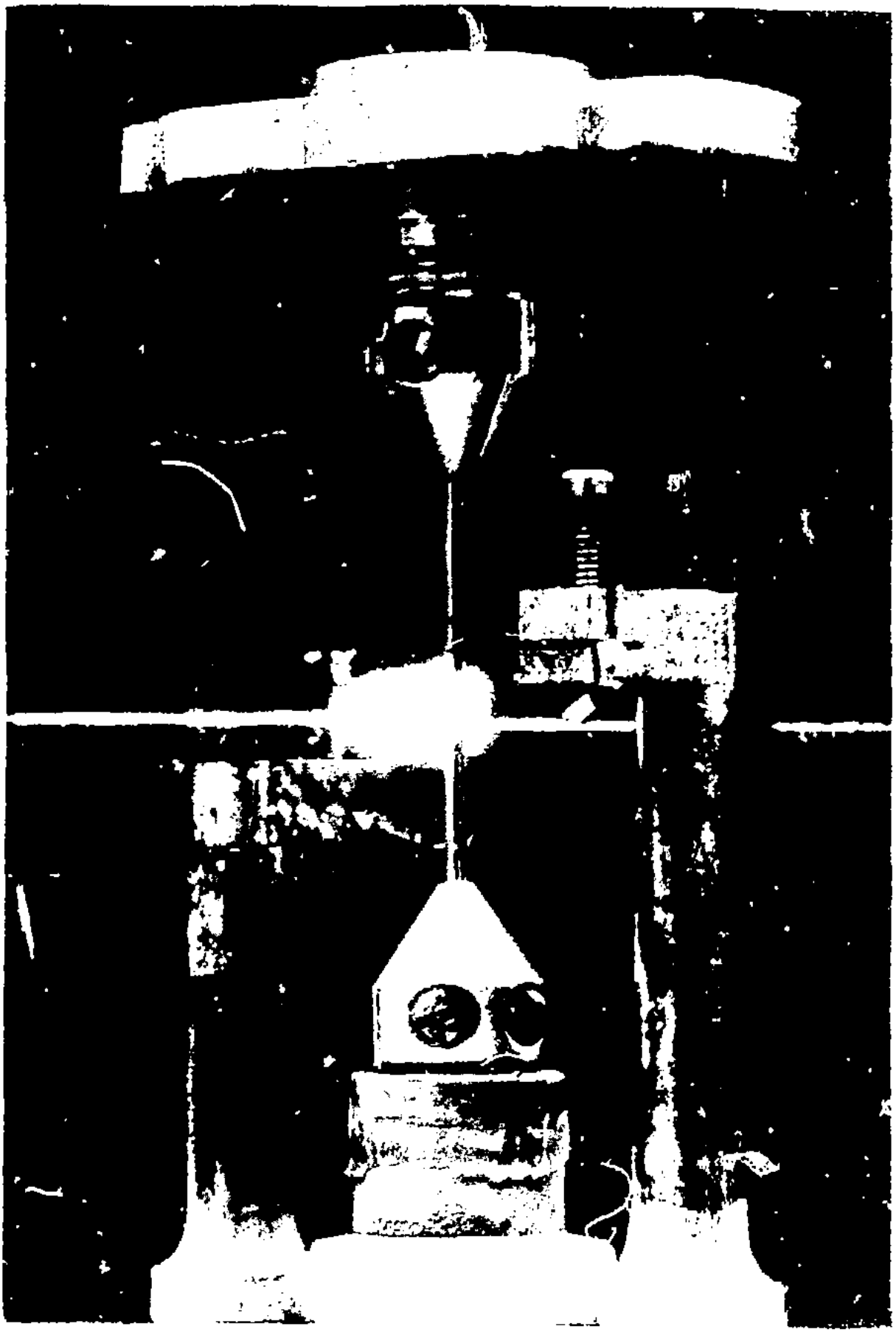

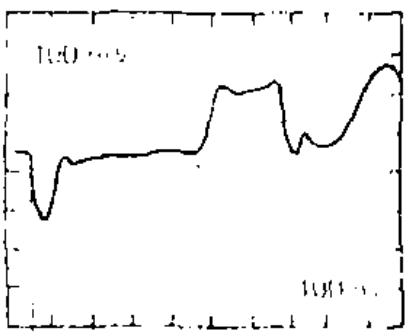
100 ns

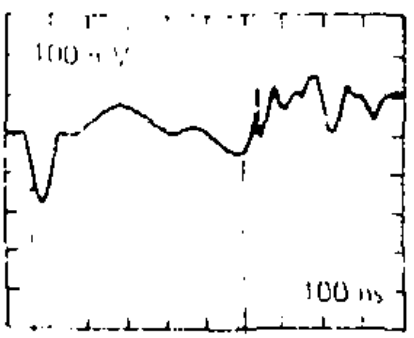
100 ns

A. Induced flaw

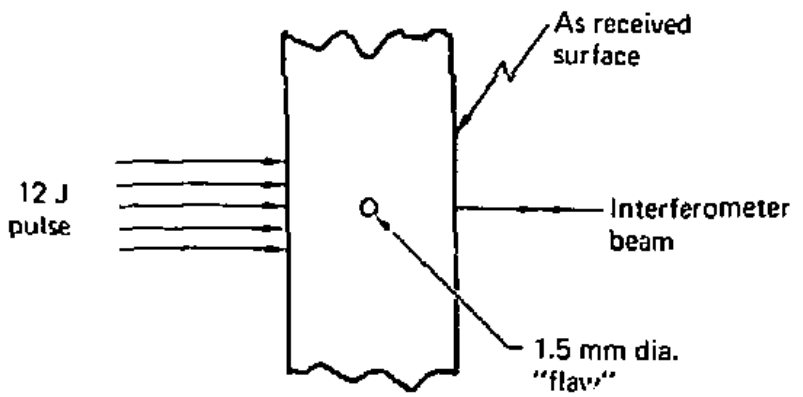

B. Flaw echo response

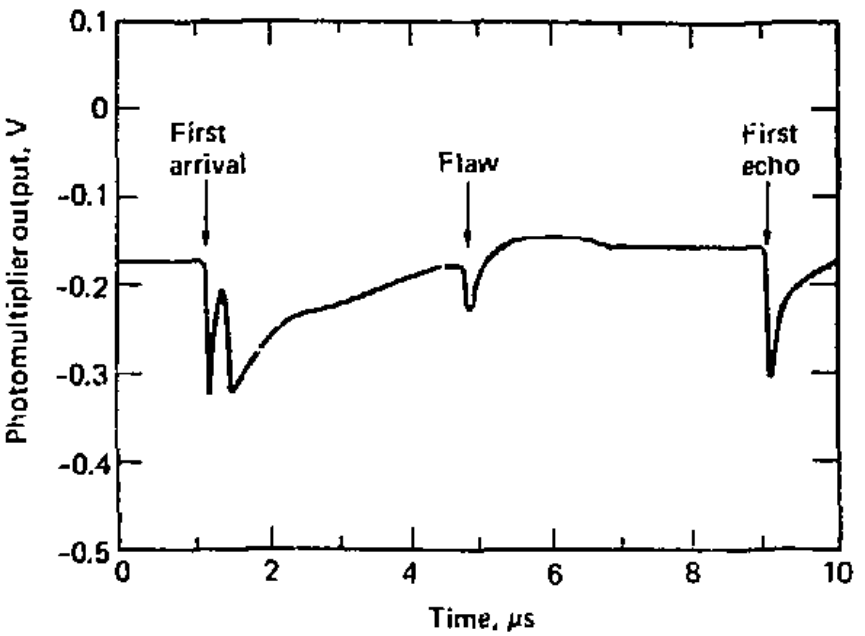

FIG. 11